

ICSV14

Cairns • Australia
9-12 July, 2007



TIME-DOMAIN ACOUSTIC SIMULATION OF 3D LINED DUCTS WITH FLOW USING AN UNSTRUCTURED DISCONTINUOUS GALERKIN METHOD

Yves Reymen, Martine Baelmans, Wim Desmet

Department of Mechanical Engineering
Katholieke Universiteit Leuven
Belgium

yves.reymen@mech.kuleuven.be

Abstract

Recently the authors proposed a new formulation to impose time-domain impedance boundary conditions. In a first step, the impedance values in the frequency-domain are fitted onto template functions. In a second step, the pressure in the time-domain can be calculated analytically as the convolution of the impedance fit of the first step with the velocity, approximated as a constant or linear function.

The resulting formulation can be written in a recursive form which makes it very efficient. It requires only some additions and multiplications; the storage is limited to one value per template in the fit. The impedance model can be guaranteed to be causal, real and passive; and is particularly suited for broadband simulations.

The formulation is implemented within the framework of an unstructured Quadrature-Free Discontinuous Galerkin Method for solving the Linearized Euler Equations. The validity of the approach has been demonstrated before for the NASA Langley Flow Impedance Tube benchmark for characterisation of lining material in a square duct without and with grazing mean flow at several frequencies. In this paper, the formulation is further validated on a more realistic case of a turbofan nacelle geometry.

1. INTRODUCTION

A mayor advantage of simulating in the time-domain is the ability to study multiple frequencies in one simulation. Here we apply an unstructured Discontinuous Galerkin Method (DGM) to study the propagation in a lined duct with varying cross-section.

A frequently used model for the propagation of acoustic waves through a mean flow are the Linearized Euler Equations (LEE). These equations account for convection and refraction effect of the (non-)uniform mean flow.

$$\frac{\partial \mathbf{q}}{\partial t} + \frac{\partial \mathbf{A}_r \mathbf{q}}{\partial x_r} + \mathbf{C} \mathbf{q} = \mathbf{s} \quad (1)$$

with quantities q (density, velocity, pressure), flux matrix A_r , gradient matrix C and sources s . These equations are solved using an unstructured DGM. Unstructured grids of tetrahedra allow to describe an arbitrary geometry, without having to make assumptions about axisymmetry or uniformity of geometry and boundary conditions.

For the simulation of a lined duct, suitable boundary conditions are needed to represent the liner material. In the time-domain this is not as straightforward as it is in the frequency-domain, where it is sufficient to impose the impedance value at the frequency of interest. In the time-domain it is necessary to prescribe the impedance for all frequencies. Every suitable formulation must comply with 3 fundamental conditions: causality, realness and passivity [1]. The 'Extended Helmholtz Resonator Model' of Rienstra was implemented by Chevaugnon and coworkers and demonstrated for 2D ducts[2]. Recently the authors proposed a time-domain impedance formulation [3, 4] suited for broadband simulations that satisfies the 3 conditions.

The DGM in combination with the time-domain impedance formulation (TDIF) has been successfully applied to the NASA Langley Flow Impedance Tube benchmark [3, 4] with hexahedral elements. Here a more complex case is studied: the propagation of a higher-order mode in a lined duct with varying cross-section [5]. The 3D geometry is an inlet of a turbofan engine with a spinner on the axis. Four types of simulations are performed on grids with tetrahedral elements: with hard or soft outer wall and with or without non-uniform mean flow.

2. DISCONTINUOUS GALERKIN METHOD

The Discontinuous Galerkin Method (DGM) can be viewed as an extension of the finite volume method by using a polynomial base to represent the quantities rather than their average value. In contrast with the finite element method, continuity between the elements is not required. The elements are independent from each other; they only communicate through a flux on their common boundaries.

2.1. General Formulation

The desired quantities q within an element are approximated by a linear combination of base functions b_k , equation (2), defined locally within an element. The contributions $q_{i,k}^e$ of each base function are the unknowns, grouped in the matrix \mathbf{q}^e . For the base functions, nodal functions are chosen. These are computed following the procedure given by Hesthaven and Warburton [6].

$$q_i^e(x, y, z, t) \cong \sum_{k=0}^{N(p,d)} q_{i,k}^e(t) \cdot b_k(x, y, z) = \mathbf{q}_i^e \cdot \mathbf{b} \quad (2)$$

The subscript i ranges over all components of the vector \mathbf{q} . For the 3D LEE there are 5 components in q . The number of base functions $N(p, d)$ is determined by the desired polynomial order p and the dimension d of the element. In case of tetrahedra it is given by $N(p, d) = (p+1)(p+2)(p+3)/6$. The size of the matrix \mathbf{q}^e is thus $5 \times N$.

For each element a Galerkin approach is obtained by multiplying the LEE by each base function and integrating over the element Ω . After application of this weighted residual formu-

lation, partial integration leads to the DG formulation, equation (3).

$$\int_{\Omega} b_k \frac{\partial q_{i,l}^e b_l}{\partial t} d\Omega - \int_{\Omega} \frac{\partial b_k}{\partial x_r} (\mathbf{A}_r \mathbf{q}^e)_i d\Omega + \int_{\partial\Omega} b_k F_{ik}^{Rn} (\bar{\mathbf{q}}^e, \bar{\mathbf{q}}^{nb}) d\partial\Omega = 0$$

$$k = 1 \text{ to } N(p, d), \quad i = 1 \text{ to } 5 \quad (3)$$

The Riemann flux F^{Rn} on the edge $\partial\Omega$ is function of the quantities in the adjacent elements e and nb . An overbar ($\bar{\cdot}$) means that the quantity is to be evaluated on the edge $\partial\Omega$.

2.2. Quadrature-Free Formulation

In principle the integration in equation (3) needs to be evaluated for each element. If each element can be mapped to a reference element Ω_{ref} , it is however sufficient to do the integration only for the associated reference element(s). For elements with straight edges, the Jacobian \mathbf{J} is a constant which makes it easy to account for the transformation from the actual coordinate system to the one of the reference element.

The formulation for an element, equation (7), is obtained by grouping together the base functions, which are functions of the spatial coordinates, and by doing the integration.

$$\left(\int_{\Omega} \mathbf{b} \mathbf{b}^T d\Omega \right) \frac{\partial \mathbf{q}^{eT}}{\partial t} - \left(\int_{\Omega} \frac{\partial \mathbf{b}}{\partial x_r} \mathbf{b}^T d\Omega \right) (\mathbf{A}_r \mathbf{q}^e)^T + \sum_{edges} \left(\int_{\partial\Omega} \mathbf{b} \bar{\mathbf{b}}^T d\partial\Omega \right) \mathbf{F}_s^{RnT} = 0 \quad (4)$$

The flux vectors can be grouped in the matrix $\mathbf{F}_r = \mathbf{A}_r \mathbf{q}^e$ and the Riemann flux vectors in the matrix $\mathbf{F}^{Rn} = 1/2((\mathbf{F}_r^e + \mathbf{F}_r^{nb})\mathbf{n}_r^{e,nb} - \alpha(\mathbf{q}^{nb} - \mathbf{q}^e))$, both of the same size as \mathbf{q}^e . The normal vector $\mathbf{n}^{e,nb}$ on the edge is taken positive in the outward direction. Notice that a Lax-Friedrich flux is used for the Riemann flux; α corresponds to the maximum eigenvalue of the $dF(q)/dq$. The Lax-Friedrich flux is one of the simplest Riemann flux formulations. It has a low operation cost, which makes it the preferred choice.

$$|\mathbf{J}_{element}| \int_{\Omega_{ref}} \mathbf{b} \mathbf{b}^T d\Omega_{ref} \frac{\partial \mathbf{q}^{eT}}{\partial t} - |\mathbf{J}_{element}| \int_{\Omega_{ref}} \frac{\partial \mathbf{b}}{\partial x_r} \mathbf{b}^T d\Omega_{ref} \mathbf{J}_{rs}^{-1} \mathbf{F}_s^T \dots$$

$$+ \sum_{edges} |\mathbf{J}_{edge}| \int_{\partial\Omega_{ref}} \mathbf{b} \bar{\mathbf{b}}^T d\partial\Omega_{ref} (\mathbf{F}^{Rn}(\bar{\mathbf{q}}^e, \bar{\mathbf{q}}^{nb}))^T = 0 \quad (5)$$

$$|\mathbf{J}_{element}| \mathbf{M} \frac{\partial \mathbf{q}^{eT}}{\partial t} - |\mathbf{J}_{element}| \mathbf{K}_r \mathbf{J}_{rs}^{-1} \mathbf{F}_s^T + \sum_{edges} |\mathbf{J}_{edge}| \mathbf{B}_{edge} (\mathbf{F}^{Rn})^T = 0 \quad (6)$$

The mass matrix \mathbf{M} , the stiffness matrix \mathbf{K}_r and the matrix \mathbf{B}_{edge} are of size $N \times N$. These matrices need only to be stored once for each element type, whereas they have to be recomputed or stored for every element in the quadrature version of the DGM. If the contributions of all the integrals over the edges are summed together in the matrix \mathbf{F}^* , one gets the following semi-discrete equation for one element:

$$\frac{\partial \mathbf{q}^{eT}}{\partial t} = \mathbf{M}^{-1} (\mathbf{K}_r \mathbf{J}_{rs}^{-1} \mathbf{F}_s^T - 1/|\mathbf{J}_{element}| \mathbf{F}^{*T}) \quad (7)$$

2.3. Properties

The quadrature-free DGM (QF-DGM) exhibits following properties:

Compactness

- adjacent elements only communicate with each other through a numerical flux.
- no global matrices need to be assembled.
- allows going high-order with unstructured grids easily.
- allows straightforward inclusion of boundary conditions.
- allows easy parallelization.

Accuracy The DGM enables to freely choose the order. Low dissipation and dispersion are characteristics of the method (lower than continuous finite element methods), even on non-uniform grids.

Efficiency The implementation makes extensive use of efficient matrix operations that maximize the work load of computer processors.

Storage Due to the discontinuous base functions, there is a higher number of degrees of freedom per element. This is partially offset by the ability to go higher-order which requires less elements for the same accuracy. Additionally, the quadrature-free formulation significantly reduces the storage requirements of the mass and stiffness matrices.

2.4. Time-Integration

The spatial discretization, the quadrature-free DGM, is advanced in time by an explicit Runge-Kutta scheme. The low-storage fourth order scheme of Carpenter [7] is used. As for every explicit scheme, the time step has to be smaller than a critical value for the simulation to be stable. This characteristic value decreases with decreasing element size and with increasing order.

3. TIME-DOMAIN IMPEDANCE FORMULATION

Most often, lining material is acoustically characterized in the frequency-domain. This is usually done by setting up a test with a single harmonic wave excitation and identifying the impedance from the forced response. The obtained complex value is the impedance at the frequency of the harmonic wave excitation. This procedure can only describe linear effects.

Time-domain computational methods have a clear advantage over frequency-domain methods for broadband problems, non-linear interaction investigations and transient wave simulations. To be able to represent an impedance boundary in the time-domain, there is a need to ‘translate’ the frequency data to the time-domain.

At a given frequency ω , the pressure $P(x_b, \omega)$ in the frequency-domain for a position x_b on the lining material, is proportional to the normal velocity $V(x_b, \omega)$ by the impedance $Z(\omega)$. A capital indicates the Fourier transform of a quantity. The equivalent expression in the time-domain involves the convolution of the inverse Fourier transform $z(t)$ of the impedance with

the velocity [1].

$$P(x_b, \omega) = Z(\omega) \cdot V(x_b, \omega) \quad (8)$$

$$p(x_b, t) = z(t) * v(x_b, t) = \int_{-\infty}^{\infty} z(\tau) \cdot v(x_b, t - \tau) d\tau \quad (9)$$

The time-domain impedance formulation proposed in references [3, 4] uses a 2-step approach. In a first step, the impedance values in the frequency-domain are fitted onto template functions. In a second step the pressure in the time-domain can be calculated analytically as the convolution of the impedance fit of the first step with the velocity, approximated as a constant or linear function.

3.1. General Broadband Formulation

A general impedance model in the frequency-domain can be written as the sum of S single pole systems and T complex conjugate pair systems. It can be easily shown that it is causal and real. Through a proper choice of the parameters it can also be made passive.

$$Z(\omega) = \sum_{k=1}^S \frac{A_k}{i\omega + \lambda_k} + \sum_{l=1}^T \frac{C_l(i\omega) + D_l}{(i\omega + \alpha_l)^2 + \beta_l^2} \quad \lambda_k \geq 0 \quad \& \quad \alpha_l \geq 0 \quad (10)$$

$$= \sum_{k=1}^S Z_k(\omega) + \sum_{l=1}^T Z_l(\omega) \quad (11)$$

$$z(t) = \sum_{k=1}^S z_k(t) + \sum_{l=1}^T z_l(t) \quad (12)$$

The convolution of the impedance impulse response $z(t)$ with the velocity $v(t)$, equation (9), can be calculated by recursive convolution thanks to the special form of $z_k(t)$ and $z_l(t)$ and the assumption that the velocity is piecewise constant or piecewise linear within a timestep Δt [3].

The resulting formulation of the time-domain impedance using recursive convolution and a piecewise constant approximation of the normal velocity is given by

$$p(n\Delta t) = \sum_{k=1}^S A_k \psi_k(n\Delta t) + \sum_{l=1}^T \left(C_l \cdot \text{Re}\{\hat{\psi}_l(n\Delta t)\} + \frac{D_l - \alpha_l C_l}{\beta_l} \cdot \text{Im}\{\hat{\psi}_l(n\Delta t)\} \right) \quad (13)$$

$$\psi_k(n\Delta t) = v(n\Delta t) \frac{1 - e^{-\lambda_k \Delta t}}{\lambda_k} + \psi_k((n-1)\Delta t) e^{-\lambda_k \Delta t} \quad (14)$$

$$\hat{\psi}_l(n\Delta t) = v(n\Delta t) \frac{1 - e^{(-\alpha_l + i\beta_l)\Delta t}}{\alpha_l - i\beta_l} + \hat{\psi}_l((n-1)\Delta t) e^{(-\alpha_l + i\beta_l)\Delta t} \quad (15)$$

where ψ_k and $\hat{\psi}_l$ are accumulators; the first is real, the second is a complex value. The formulation with a piecewise linear approximation of the velocity is given in reference [3]. For all the results shown here, a piecewise linear approximation for the normal velocity has been used. The formulation is given for the impedance, a similar formulation for the admittance is obtained by simply interchanging the role of pressure and velocity.

3.2. Single Frequency Model

For the particular case of simulations containing only one single frequency, it is useful to have a specific model capable of matching any given impedance at that frequency. A suited frequency-domain model is the 3-parameter model, equation (16), proposed by Botteldooren[8] and Tam & Auriault[9] and also used by Ju & Fung[10]. It can be considered as a mass-spring-damper model; all parameters Z_i have to be positive to fulfill the 3 fundamental conditions[1]. To be able to apply recursive convolution to this model, it is necessary to work with the admittance A , the inverse of the impedance. The model can then be written in the form of a second order model ($S = 0, T = 1$). Equation (18) gives the relation between the parameter sets $C_1, D_1, \alpha_1, \beta_1$ and Z_1, Z_0, Z_{-1} .

$$Z(\omega) = Z_{-1}/(i\omega) + Z_0 + Z_1(i\omega) = \frac{(i\omega)^2 Z_1 + (i\omega) Z_0 + Z_{-1}}{i\omega} \quad (16)$$

$$A(\omega) = \frac{1}{Z(\omega)} = \frac{C_1(i\omega) + D_1}{(i\omega + \alpha_1)^2 + \beta_1^2} \quad (17)$$

$$C_1 = 1/Z_1 \quad D_1 = 0 \quad \alpha_1 = Z_0/(2Z_1) \quad \beta_1 = \sqrt{Z_{-1}/Z_1 - \alpha_1^2} \quad (18)$$

At a design frequency $\bar{\omega}$, the impedance Z is given by the complex number $R + iX$. R is the resistance and X the reactance. Equation (19) gives the link between R, X and Z_1, Z_0, Z_{-1} from the 3-parameter model. The relation between R and Z_0 is straightforward. X has to be somehow distributed over Z_1 and Z_{-1} , while keeping the last two positive for a physically possible model. Here the choice is made to attribute a factor g of the absolute value of the reactance to one of the two Z -parameters and a matching value to the other depending on the sign of the reactance, see equation (20). The factor g has to be positive to make sure Z_1 and Z_{-1} are positive. An additional condition on g follows from the expression for β : g has to be big enough for β to be real. After some algebra the condition becomes $g \geq (-1 + \sqrt{1 + (R/X)^2})/2$.

$$Z(\bar{\omega}) = R + iX = Z_0 + i(Z_1 \bar{\omega} - Z_{-1}/\bar{\omega}) \quad (19)$$

$$\begin{aligned} Z_0 = R, \quad Z_1 = \frac{(1+g)|X|}{\bar{\omega}} \text{ and } Z_{-1} = g|X|\bar{\omega} \text{ if } X > 0 \quad \text{or} \\ Z_1 = \frac{g|X|}{\bar{\omega}} \text{ and } Z_{-1} = (1+g)|X|\bar{\omega} \text{ if } X < 0 \end{aligned} \quad (20)$$

3.3. Properties

The formulation exhibits following properties:

Efficiency The formulation requires just a few additions and multiplications per time step.

Low storage Storage is needed only for the accumulators in the boundary points. No time history of solution data is required.

Easy implementation There are no (high-order) time derivatives in the formulation, which allows it to be incorporated in all discretization schemes.

Broadband formulation The model gives sufficient freedom to approximate any set of sampled impedance values.

4. INLET TURBOFAN CASE

So far the combination of the DGM and the impedance formulation has been applied to the NASA Langley Flow Impedance Tube benchmark [3, 4]. An example of a geometrically more complex case is the inlet of a turbofan engine. Rienstra and Eversman [5] give a description of such a geometry inspired by the geometry of the successful engine design CFM56, see figure 1a. Worth noting is the presence of a spinner which significantly increases the geometrical complexity.

4.1. Description

The aim of the Rienstra-Eversman analysis is to study how modes travel through this duct and to compare the multiple scales and finite-element solution in the frequency-domain on a 2D axisymmetric model for 4 configurations: fully reflecting outer wall(hard wall) or lined outer wall(soft wall) combined with or without non-uniform mean flow characterized by a Mach number of approximately -0.5 . All quantities mentioned are non-dimensionalized. The lining is modelled by specifying a frequency-independent impedance of $2 - i$ and the mean flow is calculated analytically by the one-dimensional gas flow equations [11].

In our 3D model, figure 1a, the geometry is enlarged at both inlet and outlet by a constant section extension to impose proper boundary conditions. At the inlet a damping zone is used to introduce the annular modes; annular because of the spinner, and to damp any possible reflections. The first radial spinning mode is used as an excitation. The circumferential order is 10 and the circular frequency 16. At the outlet, a damping zone damps out the modes. Both zones are terminated by characteristic boundary conditions. At the spinner and in case of a hard outer wall a fully reflecting condition is imposed; on a soft outer wall the impedance formulation for a single frequency, as discussed above, is used. No corrections are made to the impedance in the case with a soft wall and a mean flow. The Myers' correction recently has been shown to be unstable[2]. For all simulations a similar tetrahedral mesh is used. Figure 1b only shows

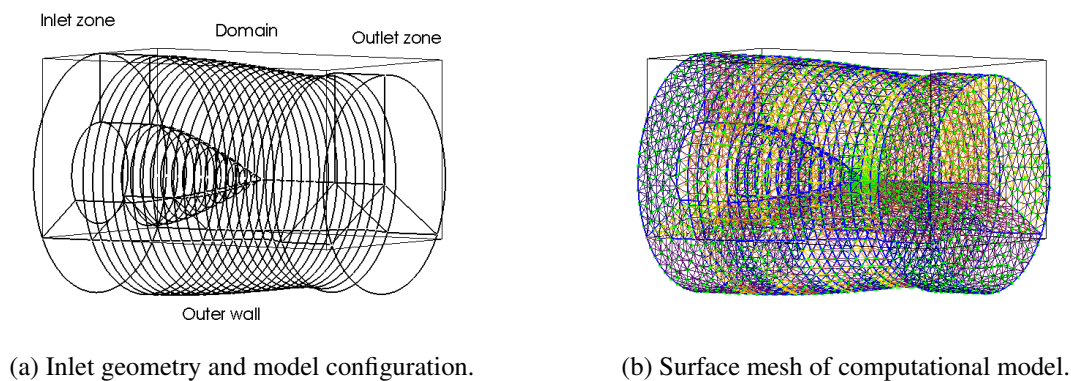


Figure 1. Inlet of Turbofan: model configuration and mesh

the surface mesh for clarity. The edges of an element are about 0.1, except near the tip of the spinner where a finer resolution of 0.01 is needed to accurately describe the geometry. Good accuracy can be obtained by working with polynomial base functions of order 2. The timestep is $1.5 \cdot 10^{-3}$ for the runs without flow and $1 \cdot 10^{-3}$ for the ones with flow. The small elements significantly reduce the time step, as it is directly proportional to the element size. A way to

relief this constraint is to use p-adaptivity [12].

4.2. Results

The solutions are postprocessed for visualization on a 51×101 grid of points on a cut along the duct axis. 51 points are equally distributed over each radial line and 101 along the duct. Results for the four cases are shown in figure 2. The instantaneous pressure is shown for the 4 cases at the end of the simulation. For the cases without flow this is $t = 5$. For the cases with flow this is $t = 8$ as it takes an acoustic wave twice as long to travel through the duct against the flow.

From the figures, it is clear that a large effect of the flow is the shortening of the wavelength. The effect of the soft wall is, as to be expected, a significant reduction in amplitude. When comparing the cases with a soft wall, the case with flow has, because of the convection effect, higher amplitudes, primarily half way the axis and the outer wall.

Figure 3 shows the amplitude of the pressure for the four cases. The left column shows the multi-scale solutions obtained by Rienstra and Eversman in the frequency-domain (see figure 6 in reference [5]); the right column shows the pressure amplitudes obtained by our method in the time-domain. The results are normalized with the largest amplitude to enable easy comparison to the results of Rienstra and Eversman, with amplitudes in the interval $[0, 1]$.

The results in the left and right column look very similar. The levels have the same distribution and shape. This shows the validity of the followed approach: quadrature-free Discontinuous Galerkin combined with the time-domain impedance formulation as introduced above.

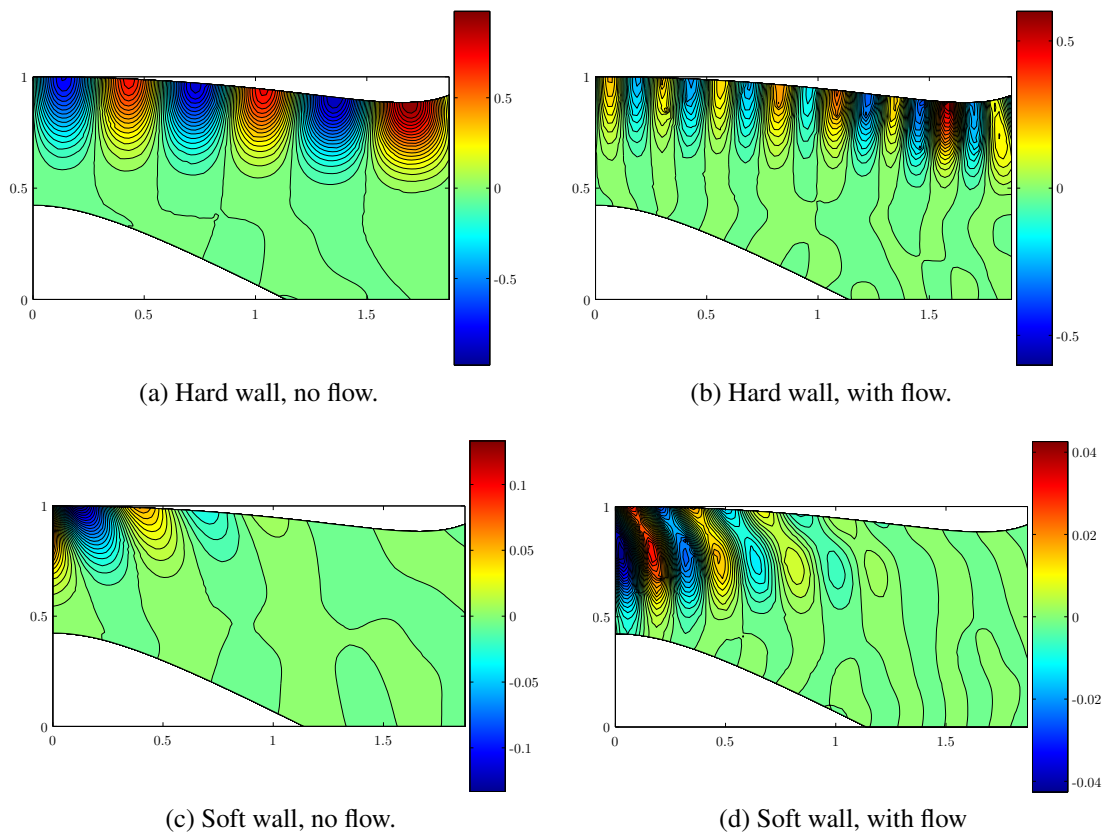


Figure 2. Iso-pressure contours at end of simulations.

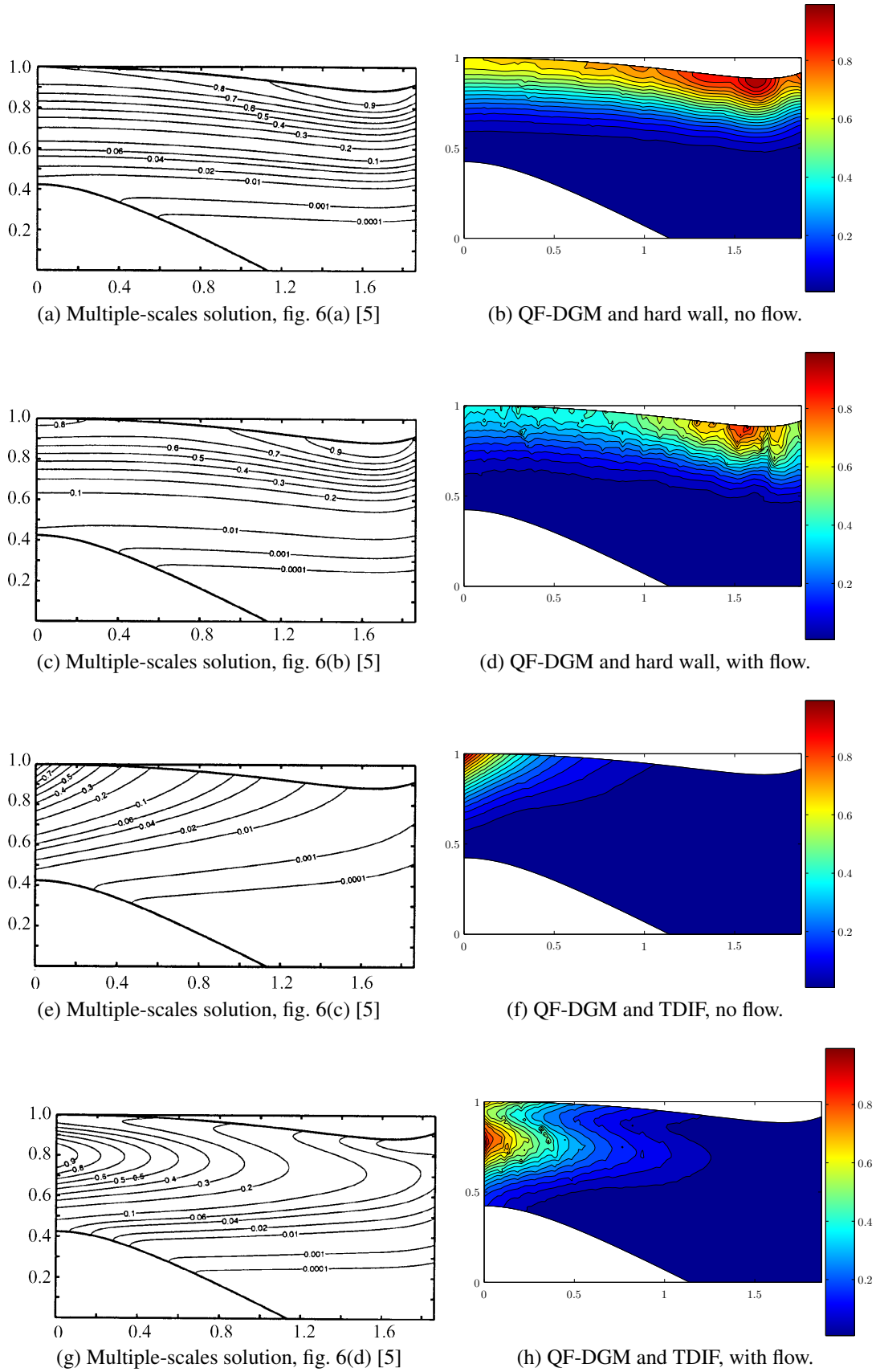


Figure 3. Comparison of iso-contours of pressure amplitudes: **first row**: hard wall, no flow; **second row**: hard wall, with flow; **third row**: soft wall, no flow; **fourth row**: soft wall, with flow.

5. CONCLUSIONS

The quadrature-free Discontinuous Galerkin Method for the Linearized Euler Equations is applied in combination with a time-domain impedance formulation to the study of propagation of modes in ducts for 4 different cases: hard or soft wall and with or without flow. The results were favorably compared with the results of Rienstra and Eversman, thus validating the followed approach. The tools developed allow to simulate complex lined geometries in three dimensions with high accuracy.

The results shown here illustrate the steps undertaken so far in the exploration of the capabilities of the QF-DGM on hexahedral and tetrahedral grids in combination with the time-domain impedance formulation. Further research needs to be undertaken to study the possibility of predicting propagation of broadband signals in a single time-domain simulation, for arbitrary geometries.

ACKNOWLEDGEMENTS

The research of Yves Reymen is funded by a fellowship of the Institute for the Promotion of Innovation through Science and Technology in Flanders (IWT-Vlaanderen).

REFERENCES

- [1] Rienstra, S., "Impedance Models in Time Domain, Including the Extended Helmholtz Resonator Model", *Proceedings of the 12th AIAA/CEAS Aeroacoustics Conference*, AIAA paper 2006-2686.
- [2] Chevaugeon, N., Remacle, J.-F., Gallez, X., "Discontinuous Galerkin Implementation of the Extended Helmholtz Resonator model in Time Domain", *Proceedings of the 12th AIAA/CEAS Aeroacoustics Conference*, AIAA paper 2006-2569.
- [3] Reymen, Y., Baelmans, M., Desmet, W., "Time-Domain Impedance Formulation based on Recursive Convolution", *Proceedings of the 12th AIAA/CEAS Aeroacoustics Conference*, AIAA paper 2006-2685.
- [4] Reymen, Y., Baelmans, M., Desmet, W., "Time-Domain Impedance Formulation suited for Broadband Simulations", *Proceedings of the 13th AIAA/CEAS Aeroacoustics Conference*, AIAA paper 2007-3519.
- [5] Rienstra, S., Eversman, W., "A numerical comparison between the multiple scales and finite-element solution for sound propagation in lined flow ducts.", *Journal of Fluid Mechanics*, **437**, pp. 367-384(2001).
- [6] Hesthaven JS, Warburton T., "Nodal high-order methods on unstructured grids: I Time-domain Solution of Maxwell's equations.", *Journal of Computational Physics*, **181**:186-221(2002).
- [7] Carpenter, M.H. , Kennedy, C.A., "A fourth-order 2N-storage Runge-Kutta scheme", *NASA TM 109112*, June, (1994).
- [8] Botteldooren, D., "Finite-difference time-domain simulation of low-frequency room acoustic problems". *Journal of the Acoustical Society of America*, Vol. 98, No. 6, 1995.
- [9] Tam, CKW, Auriault, L., "Time-Domain Impedance Boundary Conditions for Computational Aeroacoustics", *AIAA Journal*, Vol. **34**, No. 5, pp. 917-923(1996).
- [10] Ju, H., Fung, K.-Y., "Time-Domain Impedance Boundary Conditions with Mean Flow Effects", *AIAA Journal*, Vol. **39**, No. 9, pp. 1683-1690(2001).
- [11] Rienstra, S., "Sound transmission in slowly varying circular and annular ducts with flow", *Journal of Fluid Mechanics*, **380**, pp. 279-296(1999).
- [12] Chevaugeon, N., Hillewaert, K., Gallez, X., Ploumhans, P., Remacle, J.-F., "Optimal numerical parameterization of discontinuous Galerkin method applied to wave propagation problems", *Journal of Computational Physics*, **223**, pp. 188-207(2007).